Fitness tradeoffs between spores and nonaggregating cells can explain the coexistence of diverse genotypes in cellular slime molds

Corina E. Tarnita[a,1,2], Alex Washburne[a,b,1], Ricardo Martinez-Garcia[a], Allyson E. Sgro[b,c], and Simon A. Levin[a,2]

[a]Department of Ecology and Evolutionary Biology, [b]Lewis-Sigler Institute for Integrative Genomics, and [c]Joseph Henry Laboratories of Physics, Princeton University, Princeton, NJ 08544

Contributed by Simon A. Levin, December 18, 2014 (sent for review June 30, 2014)

Cellular slime molds, including the well-studied *Dictyostelium discoideum*, are amoebae whose life cycle includes both a single-cellular and a multicellular stage. To achieve the multicellular stage, individual amoebae aggregate upon starvation to form a fruiting body made of dead stalk cells and reproductive spores, a process that has been described in terms of cooperation and altruism. When amoebae aggregate they do not perfectly discriminate against nonkin, leading to chimeric fruiting bodies. Within chimeras, complex interactions among genotypes have been documented, which should theoretically reduce genetic diversity. This is however inconsistent with the great diversity of genotypes found in nature. Recent work has shown that a little-studied component of *D. discoideum* fitness—the loner cells that do not participate in the aggregation—can be selected for depending on environmental conditions and that, together with the spores, they could represent a bet-hedging strategy. We suggest that in all cellular slime molds the existence of loners could resolve the apparent diversity paradox in two ways. First, if loners are accounted for, then apparent genotypic skew in the spores of chimeras could simply be the result of different investments into spores versus loners. Second, in an ecosystem with multiple local environments differing in their food recovery characteristics and connected globally via weak-to-moderate dispersal, coexistence of multiple genotypes can occur. Finally, we argue that the loners make it impossible to define altruistic behavior, winners or losers, without a clear description of the ecology.

Dictyostelium discoideum | cooperation | dispersal | coexistence | variable environments

The cellular slime molds, of which the most studied is *Dictyostelium discoideum*, arise from starving amoebae. Upon exhausting their local supply of food, amoebae initiate a developmental program, joining with neighbors to form an aggregate. The culmination of development is a fruiting body made of stalk and spores (1–4). In nature, there is significant diversity and coexistence of multiple species and genotypes of cellular slime molds (5, 6). Moreover, chimeras (aggregates consisting of at least two genotypes) occur naturally (5–8), which implies that amoebae do not discriminate perfectly in the process of aggregation. These chimeras are functional and viable: Their aggregation results in a fruiting body in which the multiple genotypes participate both in stalk formation and in spore production, although not necessarily in equal measures, which is known as reproductive skew (7). Certain genotypes are disproportionately represented in the spores despite being equally represented in the initial population of starving amoebae, and those are considered to be stronger competitors. Studies to date have found significant reproductive skew in chimeras of a variety of cellular slime molds (9), with perhaps the greatest skew being registered for *D. discoideum*, where linear hierarchies of competitors have been described (10, 11).

In the absence of additional frequency-dependent processes that maintain coexistence, these findings point toward a decrease in genetic diversity that is inconsistent with the immense diversity and coexistence among strains in nature (9, 10). An explanation for coexistence that was suggested but unexplored both for *D. discoideum* (10) and for other cellular slime molds (9) is that strains that are at a disadvantage in chimeras have an advantage at a different stage in their life cycle, i.e., that there is a tradeoff between sporulation efficiency and other fitness-related traits. To date, analyses of genotypical fitness have focused on spore contribution as the sole fitness indicator. However, during the social phase, not all cells aggregate; some cells stay behind. We refer to such cells as nonaggregators or loners. Loner cells have been generally ignored because they were assumed to simply die (10), but recent results show that loner cells of *D. discoideum* are viable, meaning that they can eat and divide if food is replenished in the environment, and that therefore the loners can be an important component of *D. discoideum* fitness (12).

This finding fits into a long-standing theory of spatially and/or temporally heterogeneous (variable) environments leading to bet-hedging or long-term optimization strategies including dormancy versus dispersal, persistence versus normal growth versus dormancy, and exploitation versus exploration, well established in ecology from studies of plants (13–19) to those of bacteria (20–22), planktonic copepods (23), and even social insects (24). In the case of cellular slime molds, loner cells can act as a form of exploitation strategy: Certain environments may become advantageous quickly and, unlike spores that take time to

Significance

Cellular slime molds, including *Dictyostelium discoideum*, are amoebae whose life cycle includes both single-cellular and multicellular stages, the latter achieved when individual amoebae aggregate upon starvation. In the (not necessarily clonal) aggregate, there is strong selection to be represented in the reproductive spores. This would lead to a reduction in overall genotypic diversity inconsistent with the great diversity found in nature. We suggest that cells that fail to aggregate provide an additional fitness component that can resolve the inconsistency: Strong selection for aggregation only occurs in environments where food is slow to replenish. Otherwise, there is strong selection for unicellularity. These tradeoffs allow a multitude of genotypes to coexist when many environments with different food-recovery characteristics are connected via weak-to-moderate dispersal.

Author contributions: C.E.T. designed research; C.E.T., A.W., R.M.-G., and S.A.L. performed the theoretical analysis; A.E.S. performed the experiments; and C.E.T. wrote the paper with input from all authors.

The authors declare no conflict of interest.

[1]C.E.T. and A.W. contributed equally to this work.

[2]To whom correspondence may be addressed. Email: ctarnita@princeton.edu or slevin@princeton.edu.

This article contains supporting information online at www.pnas.org/lookup/suppl/doi:10.1073/pnas.1424242112/-/DCSupplemental.

germinate, loner cells can begin to eat and divide instantaneously, thus giving their genotype a head start. Then, environments where food replenishes faster (henceforth fast-recovery environments) will select for genotypes that are more likely to invest in loners, whereas environments where food replenishes slower (henceforth slow-recovery environments) will select for genotypes that are more likely to invest in spores (12).

Here we suggest that for cellular slime molds for which loners exist and are indeed part of the survival strategy of a genotype, they can contribute toward the understanding of chimeric interactions and genotypic diversity in two ways. First, we claim that the reproductive skew observed within the spores of chimeras might be only apparent and simply due to different investments into loners versus aggregating cells, and not due to chimeric interactions between genotypes. Second, assuming that there are no chimeric interactions among genotypes, we claim that if both spores and loners are part of cellular slime mold survival strategies, then many diverse genotypes can coexist in an ecosystem consisting of multiple local environments with different food-recovery characteristics, connected via weak-to-moderate dispersal. This claim relies on principles already established in ecology: When fitness has multiple components, tradeoffs between them can lead to coexistence of strategies in spatially or temporally heterogeneous environments (reviewed in refs. 25–29). In addition to these main results, we also independently confirm the viability of *D. discoideum* loners via an experimental setup different from that in ref. 12.

Experimental Results

We used cells left behind during the aggregation of starving *D. discoideum* from a naturally isolated [as opposed to axenic (12)], clonal population that were allowed to form fruiting bodies on nonnutrient agar (experimental details in *Materials and Methods*). The fruiting bodies were then removed and fresh bacteria were added as a food source. This facilitated the nonaggregating cells to regrow and deplete the bacteria as expected from ref. 12 and reaggregate and go on to form normal fruiting bodies, leaving behind a population of nonaggregating cells themselves (Fig. 1). In addition to viability, this experiment confirms that there are no longer-term effects of starvation or an epigenetic effect that would prevent these nonaggregating cells from aggregating in the future under starvation conditions. Therefore, the loners can indeed constitute an important component of *D. discoideum* fitness.

Theoretical Results

Chimeric Interactions. Existing work shows no interaction between different coexisting genotypes before the aggregate stage (9). Therefore, in agreement with refs. 1 and 30, we suggest that a natural first hypothesis is that of neutrality, i.e., that no interaction occurs at the aggregate stage either, such that genotypes behave in a chimera exactly as they would in a clonal fruiting body. Then, if different genotypes have different investments in loners depending on the environments encountered, in a 50:50 initial mix of starving amoebae, genotypes that invest more in spores and less in loners will be more represented in the spores of the chimera and vice versa (Fig. 2). Because current experimental work on chimeras only counts spores (loners are generally ignored and stalk cells are experimentally hard to count), such pairings of genotypes with different loner investments would be classified as reproductively skewed and chimeric interactions would have to be invoked to explain the skew (11). We do not suggest that chimeric interactions do not occur, but only that (*i*) they are not necessary to explain the existence of a reproductive skew and (*ii*) should they exist, they cannot be inferred unless all cells are counted, including loners, cells left behind in slug trails, stalk cells, and spores. In the absence of such data, given the lack of interaction before the aggregate stage, it is natural to assume that there are no interactions in the aggregate either.

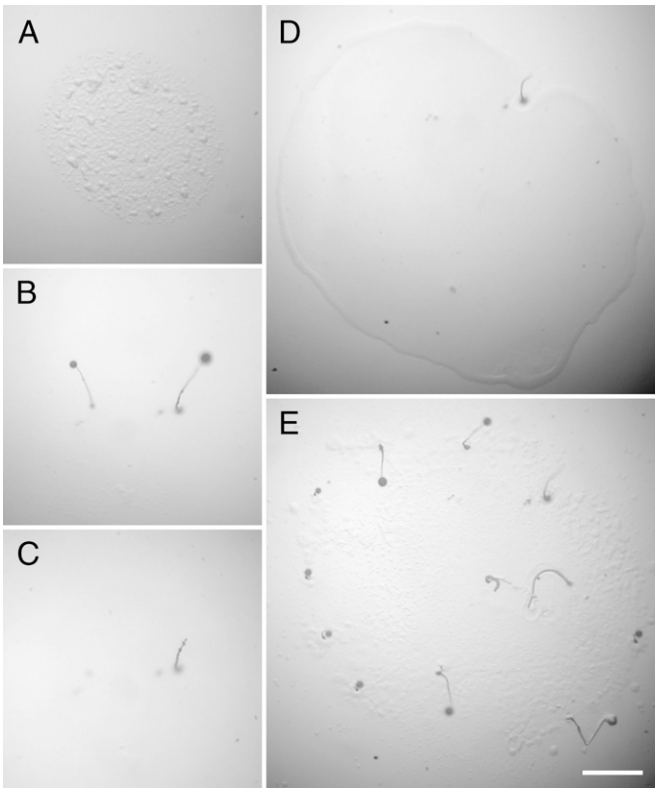

Fig. 1. "Loner" cells left behind after aggregation are fully viable and capable of aggregation during future starvation cycles. (*A*) Freshly starved cells plated on agar (day 0). (*B*) Two fruiting bodies formed from starving cells in *A* (day 2). (*C*) Fruiting bodies removed from *B*, leaving behind only stalk and loner cells (day 2). (*D*) Bacteria added to loner cells left on agar in *C* (day 2). (*E*) New fruiting bodies resulting from viable loner cells from *B*–*D* (day 5). (Scale bar, 1 mm.) At this scale, individual cells cannot be observed. This image is representative of multiple replicates run with different genotypes.

Genotypic Diversity. Next, starting from the hypothesis of no chimeric interactions, we construct a well-mixed model of resource competition similar to that of ref. 12 and extend it to explore the effect of multiple environments on genotypic diversity. Because we assume that genotypes behave in chimeras exactly as they behave when clonal, it is not necessary to model chimeras explicitly: Whether chimeras are formed or not (and how many of them are formed) becomes irrelevant to the dynamics (Fig. 2).

In our model, for simplicity, we equate genotype and phenotype. A genotype is characterized by a scalar α, which represents the fraction of cells that aggregate; the remaining $1 - \alpha$ constitute the fraction of nonaggregating cells, or loners. Thus, if $\alpha = 0$, a monoculture of genotype α does not undergo an aggregation phase; if $\alpha = 1$, a monoculture only produces aggregates and leaves no loner cells behind. Intermediate α values represent a mixed strategy, where some cells aggregate and others do not. Out of the cells that aggregate, only a fraction will become spores; the remaining cells are not viable; or they die and contribute to the formation of stalk, as is the case for *D. discoideum*; or, under environmental conditions where a migrating slug is formed, they get shed during migration. In this paper we are not concerned with the selective forces that shape the stalk-to-spore investment ratio or the average length of slug migration and therefore, for simplicity, we assume that the cell

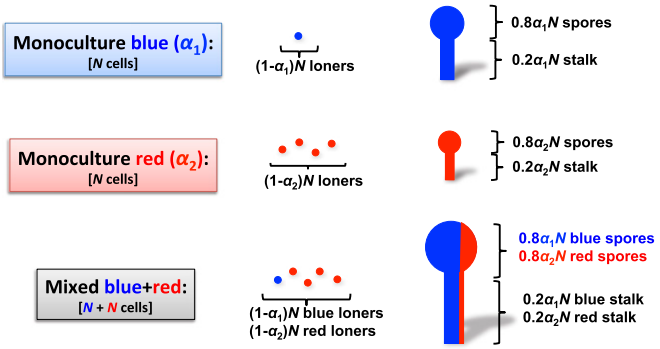

Fig. 2. Chimeric interactions are not necessary to produce reproductive skew in spores. Genotype A (blue) invests a fraction α_1 in aggregation and $(1-\alpha_1)$ in loners; genotype B (red) invests α_2 in aggregation and $(1-\alpha_2)$ in loners. Of the aggregating cells, 20% become stalk and 80% spores. Then, (*i*) if A is clonal (*N* initial cells), we should observe: $(1-\alpha_1)N$ loners and a fruiting body with $0.2\alpha_1 N$ stalk cells and $0.8\alpha_1 N$ spore cells; (*ii*) if B is clonal (*N* initial cells), we should observe: $(1-\alpha_2)N$ loners and a fruiting body with $0.2\alpha_2 N$ stalk cells and $0.8\alpha_2 N$ spore cells; and (*iii*) if *N* A cells and *N* B cells are plated together, and assuming there are no interactions in the chimera so that the two genotypes contribute to the stalk and spores exactly as they would within clonal aggregates, then we should observe: $(1-\alpha_1)N$ A + $(1-\alpha_2)N$ B loners and a chimeric fruiting body with stalk = $(0.2\alpha_1 N$ A + $0.2\alpha_2 N$ B) and a spore mass = $(0.8\alpha_1 N$ A + $0.8\alpha_2 N$ B). Unless $\alpha_1 = \alpha_2$, the chimeric spore investment appears skewed, but the same skew is also present in the stalk and is simply accounted for by the differences in loner versus spore investment between genotypes.

loss during migration and the investment in the stalk are fixed and identical for all genotypes of a species. Consequently we focus our analysis solely on the fraction of spores versus loner cells.

The model we describe depends on the ecology that influences the lifecycle of the cellular slime molds. For simplicity, we are not concerned with soil type, light, or moisture and assume those to be the same across environments; the property of interest is the ability of food to replenish in a given environment or, in other words, the starvation times (times between the onset of starvation and the next resource pulse) experienced in that environment.

One environment (patch). In the first part of the model we assume that the ecosystem is comprised of a single environment, in which food replenishment can be either deterministic (certain) or stochastic (uncertain). This model is similar to that in ref. 12 but it is more general in that it explicitly accounts for resource competition among different genotypes. The amoebae consume resources, reproduce freely, and grow at a rate governed by Michaelis–Menten kinetics (details in *SI Appendix*). There is density dependence because different genotypes compete indirectly through the existing resources, but we assume no other frequency dependence (i.e., we assume that intrinsic parameters such as the growth and aggregation rates of different genotypes are independent of the composition of the population, consistent with observations in ref. 9). We further assume that amoebae die at rate μ. Resources are depleted by the growing amoebae until they are no longer able to sustain growth, after which the amoebae enter a starvation phase. During this phase, a fraction α of cells of genotype α aggregate with the purpose of forming spores, whereas the remaining $1-\alpha$ stay as starving loners. The nonaggregating (loner) cells stop consuming resources, stop reproducing, and decay at rate μ until the next resource pulse. Of the aggregating cells, a fraction s become viable spores; we assume that spores are very resistant to environmental stress, but that they nevertheless incur a small decay rate δ; therefore, we assume that $\delta < \mu$.

When the starvation period is over, food is reintroduced in one resource pulse, R_0. Then the surviving loner cells start consuming resources and reproducing immediately, whereas spores undergo a delay period τ, which is the time required to activate the metabolic machinery necessary for resource consumption. The longer the delay τ, the more cost will be incurred by spores in an environment where loner cells are already consuming the resource while the spores undergo the germination process. Therefore, genotypes that can leave behind some loners can have a head start and be favored. If resources get depleted before the germination period is over, we assume that spores return to dormancy, without incurring any cost associated with the abortion of the germination process. In reality, in addition to the costly delay of germination, certain species like *D. discoideum* also experience a costly delay of sporulation: After only 6 h, just as individual amoebae are beginning to aggregate, they are irreversibly committed to continuing with sporulation for the remaining 18 h of the process (31). Because we are trying to show that in certain environments loners can be selected for, an additional cost for the spores will only make the selection for loners stronger and reinforce our results. Therefore, for simplicity, we do not include in our model the additional cost due to the irreversibility of the sporulation process. The dynamic equations describing the spores and loners are presented in *SI Appendix*.

In a single environment as described above, with competing cellular slime mold genotypes and instantaneous, identical resource pulses arriving at random times, we explore how the lengths of the starvation periods (time between the onset of starvation and the next resource pulse) determine the winning genotype. Our results agree with those in ref. 12 and in general with well-established results in the bet-hedging literature. In a deterministic environment (i.e., when the starvation times are always of the same length) there is selection for one of the pure strategies: We find a critical threshold starvation time T_{cr} such that for $T < T_{cr}$, the winning genotype is one that never produces any aggregates ($\alpha = 0$), whereas for $T > T_{cr}$, the winning genotype is one that always aggregates to produce spores ($\alpha = 1$). When the environment is stochastic such that successive starvation times are independent and exponentially distributed with rate $1/\lambda_T$, we find that mixed strategies can be selected for: If on average the environment is a fast-recovery one (low λ_T), then the mixed strategy invests more in loners than in spores; indeed, for sufficiently low λ_T, only loners will survive. Conversely, if the environment is a slow-recovery one (high λ_T), then the mixed strategy invests more in spores, and for sufficiently high λ_T, only spores will persist (Fig. 3*A* and *SI Appendix*, Fig. S2*A*). We confirm that the winning strategy is continuously stable (32): It cannot be invaded by any rare mutant and can invade any resident monoculture from rare initial levels (*SI Appendix*, Fig. S2*B*). Here we assume an exponential distribution of starvation times; assuming uniformly distributed starvation times leads to qualitatively similar results (12). In the future, it will be interesting to explore other distributions (e.g., normal); however, we generally expect similar results to hold.

The effects of the model parameters on the evolutionarily stable genotype are intuitive: The higher the consumption rate c, and implicitly the reproductive rate of solitary amoebae, the longer the costly spore germination delay τ, and the higher the death rate of spores, δ, the more the loners will be favored. Conversely, the higher the spore success rate s or the death rate of solitary cells μ, the more spores will be favored. Finally, varying the fixed resource pulse R_0 in a stochastic environment has little effect on the winning genotype. A detailed sensitivity analysis can be found in *SI Appendix*, Figs. S3 and S4.

Multiple environments (patches). In this part, we explore whether the extension of our model to a spatially heterogeneous ecosystem with multiple local environments connected via spore dispersal can, under certain conditions, favor the coexistence of a diverse range of genotypes. We consider $M = 25$ stochastic environments evenly spanning the range of average starvation

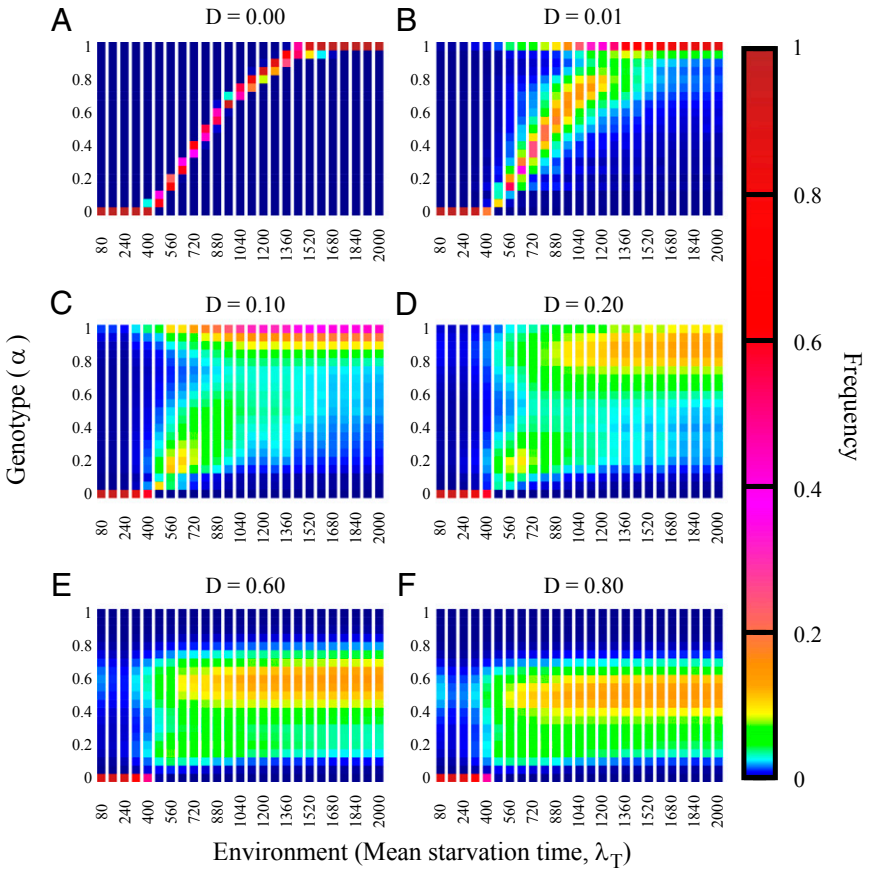

Fig. 3. Different environments connected via weak-to-moderate dispersal, *D*, can maintain coexistence of genotypes. Mean genotype frequency of 21 genotypes ($\alpha = 0.05i$; $i = 0,\ldots,20$) in 25 environments. Average is taken over 60 replicates after 1,500 growth/starvation cycles in the slowest environment. (*A*) Without dispersal, stochastic starvation times can select for mixed strategies but no coexistence. In each environment, there is only one evolutionarily stable strategy. The surviving genotype in the simulations alternates between both highlighted genotypes in the figure due to the discretization in α. The actual winning strategy is one in between (details in *SI Appendix*). (*B–E*) In multiple environments, if food recovery is stochastic and the environments are sufficiently different, coexistence between a multitude of strategies is possible for weak-to-moderate dispersal. (*F*) For high dispersal, coexistence will tend to be lost—one winning genotype emerges, which bet hedges over all existing genotypes. Parameters are as in *SI Appendix*, Table S1. The colors correspond to frequencies such that dark blue = 0–0.0075; blue = 0.0075–0.025; green = 0.025–0.05; yellow = 0.05–0.0875; orange = 0.0875–0.125; magenta = 0.125–0.375; red = 0.375–0.625; and dark red = 0.625–1. Transitions between colors are given by gradients.

times from $\lambda_T = 80$ (which in the absence of dispersal selects for all loners) to $\lambda_T = 2{,}000$ (which in the absence of dispersal selects for all spores) (Fig. 3*A*). Each environment is governed by the same dynamics as above, but they receive and exhaust resources independently of each other (asynchronously); the only element that couples the dynamics of the environments is the dispersal of spores. When starvation occurs in an environment, a fraction $1 - D$ of the spores remains in the home environment, whereas a fraction D is dispersed uniformly across the other environments. Because the dynamics in the environments are desynchronized, when spores get moved to a new environment they may immediately find food and start the germination process, or they may be lying dormant until food gets introduced into that environment.

In the absence of dispersal, each environment will have its winner, as discussed above in *One Environment (Patch)*; and the more different the environments, the more different the respective winning genotypes (Fig. 3*A*). When dispersal connects the environments, for low values of D, a multitude of genotypes coexists in almost all environments; this is consistent with theory (25). The most abundant genotypes in each environment are those close to the genotype for which that environment selects in the absence of dispersal; however, many other diverse genotypes coexist, albeit at lower abundances (Fig. 3 *B* and *C* and *SI Appendix*, Figs. S7–S10). Overall, almost all genotypes are present in the whole ecosystem. The only environments with little-to-no coexistence are the very fast recovery environments, in which, as is the case in the absence of dispersal, the all-loner strategy is by far the most dominant genotype present. This is because in such environments, the food recovers quickly enough that the resident loners can (almost) completely consume it before any immigrant spores can finish their germination process (Fig. 3 *B* and *C*).

As dispersal increases, the environments get increasingly more connected. For intermediate dispersal, the winning strategies segregate into two subsets: one subset with higher loner investment dominating the fast-recovery environments and one subset with higher spore investment dominating the slow-recovery environments (Fig. 3*D*). When dispersal becomes high enough, there is sufficient transfer between all environments for a new successful genotype to emerge that is selected to bet hedge over the average of all existing environments (Fig. 3*F*); the two winning subsets from the intermediate dispersal region now merge (Fig. 3*E*) and coexistence is reduced only to a subset of genotypes neighboring the dominant bet hedger. These genotypes now coexist in more or less all environments, although they are still poorly represented in the fast-recovery environments where loners continue to dominate (Fig. 3*F*). Throughout, we

measure cumulative genotype frequency including both spores and loners (a breakdown can be found in *SI Appendix*, Fig. S6). Eventually, as dispersal continues to increase, we expect coexistence to be lost. In general, the dispersal range for which coexistence is maintained depends on how many and how different the environments are, with more similar environments losing coexistence at lower levels of dispersal. Our results agree with general theoretical predictions on the effect that global dispersal has on coexistence (reviewed in ref. 29).

Discussion

We argue that if loners (nonaggregating cells) are part of the cellular slime mold survival strategy, recognizing this contributes to an understanding of chimeric dynamics and genotypic diversity in two ways. First, it shows that chimeric interactions between genotypes are not necessary to produce reproductive skew in the spores of chimeras. Under the assumption of neutral interactions, the skew is accounted for by a skewed investment in loners by the two genotypes. In this case, the location of a genotype in the competitive hierarchy based on spore investment in chimeras is inversely related to the genotype's investment in loners.

Second, in the context of a richer ecology (variable food-recovery environments connected via weak-to-moderate dispersal), the loners can provide an explanation for the great genotypic diversity observed in nature. The loners—an exploitation strategy—can also be seen as fulfilling the role of local dispersal. By contrast, the spores—an insurance against prolonged starvation—also fulfill the role of global dispersal. Because environments with different food-replenishment characteristics select for different investments in spores versus loners, we showed that weak-to-moderate dispersal between faster-recovery and slower-recovery environments can allow for the coexistence of multiple genotypes (Fig. 4 provides a schematic description of our argument for two environments).

So far, only *D. discoideum* loners have been demonstrated to be viable here and elsewhere (12) but one can expect similar findings in other cellular slime molds. The viability of the loners does not demonstrate that they are part of the slime mold survival strategy and much remains to be done empirically in this direction, including work to uncover the mechanisms by which a genotype mediates the amount of loner cells left behind. The viability of loners, however, is consistent with this hypothesis, especially in the context of the vast existing theoretical and empirical literature on bet-hedging strategies in microbes.

Because quorum sensing is instrumental in the decision to aggregate in *D. discoideum* (reviewed in ref. 3), one possibility is to search for mechanistic hypotheses there. We hypothesize two related mechanisms by which a *D. discoideum* genotype could lead to mixed investment in loners and spores when grown in a monoculture: (*i*) direct, signal-mediated quorum activation and (*ii*) indirect, resource co-mediated quorum activation. The former posits the genotypes have varying and heritable sensitivities directly to the autoinducer; the latter posits that resource availability mediates a cell's probability of responding to an autoinducer and that the genotypes have varying resource starvation tolerances (hence resource co-mediated quorum activation). As resources are depleted, small-scale spatial heterogeneity can lead to some cells of the same genotype sensing abundant resources in their local environment and others sensing sparse resources. For a given level of resources and a given degree of spatial heterogeneity, a fraction of the cells may initiate their developmental program and move toward aggregation, and that fraction can vary across genotypes due to variation in the sensory and transcriptional machinery involved in detecting local resource density. Recent work (12) supports the plausibility of such a mechanism, but as loners still remain even in homogenous food conditions it is unresolved if this is the only mechanism at work in loner formation. We suggest that dose–response experiments examining different genotypes' responsiveness to the autoinducer at various resource concentrations could test this hypothesis and assess the validity of our model.

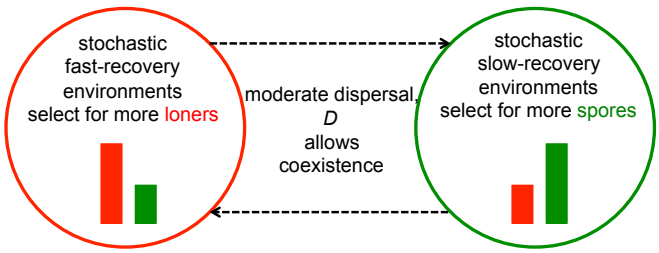

Fig. 4. Fast-recovery environments select for investment in loners; slow-recovery environments select for investment in spores. Fast- and slow-recovery environments connected via weak-to-moderate dispersal allow for coexistence of strategies—each strategy dominates its home environment but dispersal allows for it to be present in the other environment as well.

It is furthermore important to note that the spores and loners are not the only components of the amoeba fitness: Both stalk allocation and cells left behind in the trail of the slug need to be included, because the former plays a crucial role in dispersal and the latter have been shown to remain viable (33). However, because slugs are not always formed and because they travel different distances depending on the environment (therefore shedding different numbers of cells), a more careful analysis and further experiments are necessary to determine exactly how to include these additional components. Here we showed that a very simple mechanism allows for great diversity. We expect that, provided more empirical evidence, further extensions of the model to include stalk- and trail-shedding allocations and additional elements of the ecology of different environments are likely to allow for even richer dynamics and greater coexistence.

Here we have made a theoretical case for explaining the great genetic diversity of cellular slime molds through considering the nonaggregating cells. We further suggest however that, if the loners are indeed shown to be selected for, other existing analyses of cellular slime molds and in particular *D. discoideum* need to be revisited. For example, because stalk cells undergo apoptosis, *D. discoideum* has been used as a powerful model organism to explore the evolution and maintenance of altruism (reviewed in ref. 3). However, whereas before the fitness of a genotype was well defined as the number of spores it produced, because of the loners' contribution, fitness becomes a relative quantity that strongly depends on the environments that genotype will encounter. Therefore, in this context, a cheater, whether it be in a clonal or chimeric context, is much more challenging to define, motivating a comprehensive consideration of an organism's life history and ecological context when looking for problems of altruism.

Materials and Methods

Experiments. Clonal, natural strains NC34.1, NC105.1, and NC85.2 of *D. discoideum*, originally from Little Butts Gap, North Carolina (34) were obtained from dictyBase (35) and maintained on *Klebsiella aerogenes* lawns grown on SM agar plates (36). For growth of amoebae, spores of each strain were inoculated in SorMC buffer (15 mM KH_2PO_4, 2 mM Na_2HPO_4, 50 μM $MgCl_2$, and 50 μM $CaCl_2$, pH 6.0) supplemented with *Klebsiella* to an OD_{600} of 8 and shaken at 180 rpm. For starvation experiments, vegetative cells were harvested from these shaking cultures, washed, and resuspended at 1–2 × 10^7 cells per milliliter in developmental buffer (10 mM K/Na_2 phosphate buffer, 2 mM $MgSO_4$, 200 μM $CaCl_2$, pH 6.5). A total of 1–2 μL of this cell suspension was placed on a nonnutrient agar plate and allowed to aggregate. To test the viability of cells left behind after aggregation, spores were removed using tweezers, and 5 μL of *Klebsiella* at an OD_{600} of 8 in SorMC was added to the remaining cells. The results shown in Fig. 1 are for strain NC34.1.

Simulations. We performed numerical simulations of $M = 25$ patches undergoing desynchronized growth–starvation cycles. The patches were chosen with mean starvation times $\lambda_T = 80i$, $i = 1,\ldots,25$. The spectrum of genotypes was discretized: We used 21 strategies ($\alpha_i = 0.05i$, $i = 0,\ldots,20$) corresponding to a regular discretization of step 0.05 (Fig. 3). Initial abundances of each genotype were independently drawn from a standard log-normal distribution and subsequently normalized so that the entire population contained 10^8 cells in every environment. The cells of the different genotypes were then split into spores with probability α_i and loners with probability $1 - \alpha_i$. An initial resource pulse of magnitude 10^8 was added and the trajectories governed by *SI Appendix*, Eq. **1** were integrated using finite-differences numerical methods. Dispersal took place at the end of the growth phase in a given environment. First, the population of each genotype was divided into spores and loners depending on α; afterward, a fraction D of the successfully formed spores was equally distributed among the rest of the environments. The starvation phase started then in the dispersing environment, with a duration T_k drawn from the exponential distribution of that environment, with mean λ_T. During this period spore populations decayed exponentially at rate δ, whereas loners decayed exponentially at rate μ, such that $\delta < \mu$. At the end of the starvation time we measured the abundance of each genotype and a new resource pulse of size 10^8 arrived. To obtain Fig. 3, 60 realizations were run for 1,500 growth/starvation cycles in the slowest patch, which means, on average 3×10^6 h. Dispersed spores arriving to depleted patches remained dormant until a new pulse of resources arrived. If resources were still present in the new environment, the spores started germinating and became active amoebae after time τ. If resources disappeared before the germination process could be completed, then the spores aborted germination at no cost to them.

ACKNOWLEDGMENTS. We thank J. Bonachela, J. Bonner, E. Cox, and T. Gregor for many useful discussions; P. Rainey and F. Weissing for extensive comments that helped shape the manuscript; and C. Nizak and colleagues for generously sharing their work with us before publication. C.E.T., A.W., and S.A.L. acknowledge support from the Templeton Foundation Foundational Questions in Evolutionary Biology Grant RFP-12-14; A.E.S. acknowledges support from the National Institutes of Health through a National Research Service Award F32 GM103062 and an R01 GM098407; and A.W. acknowledges support from the National Science Foundation through Graduate Fellowship NSF DGE-1148900.

1. Bonner JT (2009) *The Social Amoebae: The Biology of Cellular Slime Molds* (Princeton Univ Press, Princeton).
2. Bonner JT (1982) Evolutionary strategies and developmental constraints in the cellular slime molds. *Am Nat* 119:530–552.
3. Strassmann JE, Queller DC (2011) Evolution of cooperation and control of cheating in a social microbe. *Proc Natl Acad Sci USA* 108(Suppl 2):10855–10862.
4. Raper KB (1984) *The Dictyostelids* (Princeton Univ Press, Princeton).
5. Fortunato A, Strassmann JE, Santorelli L, Queller DC (2003) Co-occurrence in nature of different clones of the social amoeba, *Dictyostelium discoideum*. *Mol Ecol* 12(4): 1031–1038.
6. Sathe S, et al. (2010) Genetic heterogeneity in wild isolates of cellular slime mold social groups. *Microb Ecol* 60(1):137–148.
7. Strassmann JE, Zhu Y, Queller DC (2000) Altruism and social cheating in the social amoeba *Dictyostelium discoideum*. *Nature* 408(6815):965–967.
8. Gilbert OM, Foster KR, Mehdiabadi NJ, Strassmann JE, Queller DC (2007) High relatedness maintains multicellular cooperation in a social amoeba by controlling cheater mutants. *Proc Natl Acad Sci USA* 104(21):8913–8917.
9. Sathe S, Khetan N, Nanjundiah V (2014) Interspecies and intraspecies interactions in social amoebae. *J Evol Biol* 27(2):349–362.
10. Fortunato A, Queller DC, Strassmann JE (2003) A linear dominance hierarchy among clones in chimeras of the social amoeba *Dictyostelium discoideum*. *J Evol Biol* 16(3): 438–445.
11. Buttery NJ, Rozen DE, Wolf JB, Thompson CRL (2009) Quantification of social behavior in D. discoideum reveals complex fixed and facultative strategies. *Curr Biol* 19(16): 1373–1377.
12. Dubravcic D, van Baalen M, Nizak C (2014) An evolutionarily significant unicellular strategy in response to starvation stress in *Dictyostelium* social amoebae. *F1000 Res* 3: 133.
13. Cohen D (1966) Optimizing reproduction in a randomly varying environment. *J Theor Biol* 12(1):119–129.
14. Hamilton WD, May RM (1977) Dispersal in stable habitats. *Nature* 269:578–581.
15. Levin SA, Cohen D, Hastings A (1984) Dispersal strategies in patchy environments. *Theor Popul Biol* 26:165–191.
16. Cohen D, Levin SA (1987) The interaction between dispersal and dormancy strategies in varying and heterogeneous environments. *Mathematical Topics in Population Biology, Morphogenesis, and Neurosciences*, eds Teramoto E, Yamaguti M (Springer, Heidelberg), pp 110–122.
17. Campbell BD, Grime JP, Mackey JML (1991) A trade-off between scale and precision in resource foraging. *Oecologia* 87:532–538.
18. Cohen D, Levin SA (1991) Dispersal in patchy environments: The effects of temporal and spatial structure. *Theor Popul Biol* 39:63–99.
19. Ludwig D, Levin SA (1991) Evolutionary stability of plant communities and the maintenance of multiple dispersal types. *Theor Popul Biol* 40:285–307.
20. Kussell E, Kishony R, Balaban NQ, Leibler S (2005) Bacterial persistence: A model of survival in changing environments. *Genetics* 169(4):1807–1814.
21. Kussell E, Leibler S (2005) Phenotypic diversity, population growth, and information in fluctuating environments. *Science* 309(5743):2075–2078.
22. Fridman O, Goldberg A, Ronin I, Shoresh N, Balaban NQ (2014) Optimization of lag time underlies antibiotic tolerance in evolved bacterial populations. *Nature* 513(7518):418–421.
23. Hairston NG, Jr, Olds EJ (1984) Population differences in the timing of diapause: Adaptation in a spatially heterogeneous environment. *Oecologia* 61:42–48.
24. Hopper KR (1999) Risk-spreading and bet-hedging in insect population biology. *Annu Rev Entomol* 44:535–560.
25. Levin SA (1974) Dispersion and population interactions. *Am Nat* 108:207–228.
26. Tilman D, Pacala S (1993) The maintenance of species richness in plant communities. *Species Diversity in Ecological Communities*, eds Ricklefs R, Schluter D (University of Chicago Press, Chicago), pp 13–25.
27. Levin SA (2000) Multiple scales and the maintenance of biodiversity. *Ecosystems (N Y)* 3:498–506.
28. Chesson P (2000) Mechanisms of maintenance of species diversity. *Annu Rev Ecol Evol Syst* 31:343–366.
29. Amarasekare P (2003) Competitive coexistence in spatially structured environments: A synthesis. *Ecol Lett* 6:1109–1122.
30. Bonner JT (2013) *Randomness in Evolution* (Princeton Univ Press, Princeton).
31. Katoh M, Chen G, Roberge E, Shaulsky G, Kuspa A (2007) Developmental commitment in *Dictyostelium discoideum*. *Eukaryot Cell* 6(11):2038–2045.
32. Christiansen FB (1991) On conditions for evolutionary stability for a continuously varying character. *Am Nat* 138:37–50.
33. Kuzdzal-Fick JJ, Foster KR, Queller DC, Strassmann JE (2007) Exploiting new terrain: An advantage to sociality in the slime mold *Dictyostelium discoideum*. *Behav Ecol* 18: 433–437.
34. Francis D, Eisenberg R (1993) Genetic structure of a natural population of *Dictyostelium discoideum*, a cellular slime mould. *Mol Ecol* 2(6):385–391.
35. Fey P, Dodson R, Basu S, Chisholm RL (2013) One stop shop for everything *Dictyostelium*: dictyBase and the Dicty Stock Center in 2012. *Methods Mol Biol* 983:59–92.
36. Fey P, Kowal AS, Gaudet P, Pilcher KE, Chisholm RL (2007) Protocols for growth and development of *Dictyostelium discoideum*. *Nat Protoc* 2:1307–1316.

Supplementary Information: "Fitness tradeoffs between spores and non-aggregating cells can explain the coexistence of diverse genotypes in cellular slime molds"

1 Model setup and analytical results for one environment

The dynamics of free-living amoebae is described by:

$$\begin{aligned} \frac{dR}{dt} &= -\frac{cR}{R_{1/2}+R}\sum_{\alpha} X_\alpha \\ \frac{dX_\alpha}{dt} &= \frac{cR}{R_{1/2}+R}X_\alpha - \mu X_\alpha \end{aligned} \tag{1}$$

for all genotypes α. Here R is the available resource and X_α is the abundance of amoebae of genotype α. Amoebae die at rate μ and reproduce and grow following Michaelis-Menten kinetics [1], where c is chosen such that $c > \mu$. When resources are no longer able to sustain the growth of amoebae (i.e. when $dX_\alpha/dt = 0$ and $R^* = \mu R_{1/2}/(c-\mu)$), these enter a starvation phase. We let $t^*_{X_0;R_0}$ be the time to starvation when the initial total amoeba population is X_0 and the initial resource availability is R_0. For simplicity of exposition we will henceforth often use t^* (unless otherwise needed for disambiguation) but we will implicitly assume its dependence on initial conditions.

We proceed to calculate the time to starvation t^*, the total abundance of amoebae at time t, $X(t) = \sum_\alpha X_\alpha(t)$ and the abundance of amoebae of genotype α at time t, $X_\alpha(t)$. From equations (1) we obtain the change in amoeba abundance X as a function of resources

R:

$$dX/dR = -1 + \frac{\mu}{c} + \frac{\mu R_{1/2}}{cR} \tag{2}$$

which allows us to find X as a function of R, and of the initial conditions:

$$X(R; X_0; R_0) = \Big(-1 + \frac{\mu}{c}\Big) R + \frac{\mu R_{1/2}}{c} \log R + \text{const.}(X_0, R_0) \tag{3}$$

Here the constant term is determined from the initial conditions. Plugging (3) into the first equation in (1) we find

$$\begin{aligned} \frac{dR}{dt} &= -\frac{cR}{R_{1/2} + R} X \\ &= -\frac{cR}{R_{1/2} + R} \left(\Big(-1 + \frac{\mu}{c}\Big) R + \frac{\mu R_{1/2}}{c} \log R + \text{const.}(X_0, R_0) \right) =: -\frac{1}{f_1(R; X_0; R_0)} \end{aligned} \tag{4}$$

where the last equality simply indicates notation. Here f_1 is monotonic and positive on the interval of interest. Then we obtain an expression for time as a function of resources:

$$t(R; X_0; R_0) = \int_{R_0}^{R} \big(-f_1(y)\big) dy = \int_{R}^{R_0} f_1(y) dy =: f_2(R; X_0; R_0) \tag{5}$$

where the last equality is again notation. From this equation, which we solve via numerical integration, we obtain two key quantities. First, we find the time to starvation t^* simply as

$$t^*(X_0; R_0) = \int_{R^*_{X_0, R_0}}^{R_0} f_1(y) dy \tag{6}$$

where $R^*_{X_0,R_0}$ is the equilibrium level of resources in equation (1) with initial conditions X_0, R_0.

Second, by finding the inverse of function f_2, which exists since f_1 and hence f_2 are strictly monotonic functions of R, we obtain R as a function of t:

$$R(t; X_0; R_0) = f_2^{-1}(t(R; X_0; R_0)) \tag{7}$$

From (4) we know that $X = (R_{1/2} + R)/(cRf_1(R; X_0; R_0))$, so substituting $R(t)$ we find the abundance X as a function of time:

$$X(t; X_0; R_0) = \frac{R_{1/2} + f_2^{-1}(t)}{cf_2^{-1}(t)} \frac{1}{f_1(f_2^{-1}(t))} \tag{8}$$

Because we assume that amoebae of different genotypes have identical reproductive and death rates, we can write the growth derived from one cell during time t, starting with initial population size X_0 and resources R_0 as:

$$G(t; X_0; R_0) = \frac{X(t; X_0; R_0)}{X_0} \tag{9}$$

Then the abundance of amoebae of genotype α at time t is given by $X_\alpha(t; X_0; R_0) = X_{\alpha,0} G(t; X_0; R_0)$, where $X_{\alpha,0}$ is the initial abundance of genotype α.

We can now proceed to analyze the fate of a genotype when successive periods of food and starvation occur. In what follows, to simplify our analysis, we assume that, after a starvation period, the same amount of initial resources is introduced. Moreover, in order to simplify our notation we will use t^* (but implicitly assume that it depends on the initial resources as well as the initial population size) to denote the time to starvation after all amoebae are active. If the population has a non-zero number of spores, then from the moment resources are introduced it will take time τ for all amoebae to be active. It is at that point (after time τ) that we start to measure the starvation time t^* (see Fig. S1). Because spores and loners have different fates, we keep track of each independently; furthermore, we keep track of the number and length of starvation periods that a genotype has experienced. We consider a food period followed by a starvation period as one event and we let $S_{\alpha,k}$ and $L_{\alpha,k}$ denote the abundance of spores, respectively of loners of genotype α after the kth food phase (i.e. at the beginning of the starvation phase of event k, see Fig. S1).

We distinguish two cases:

(i) the loners finish the available food before the spores have had a chance to germinate;

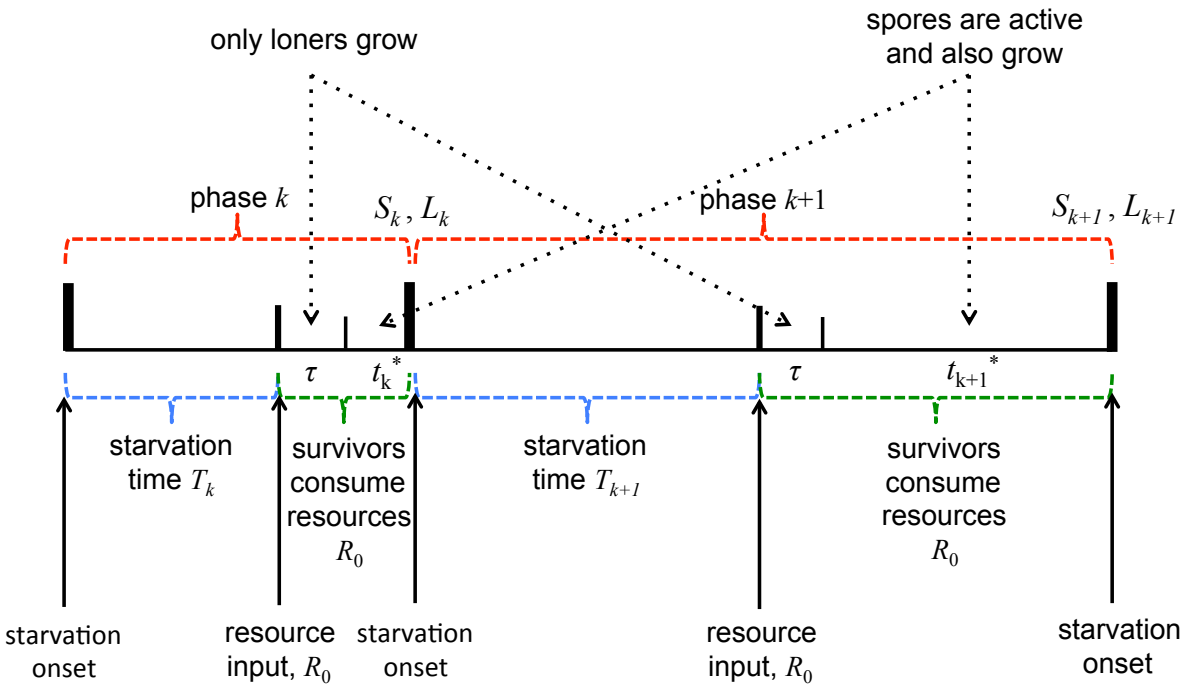

Fig. S 1 – Events k and $k+1$ with their growth and starvation phases, showing where the spores S and loners L are measured in our analytical description above. The starvation time T is measured from the onset of starvation to the following resource input.

this can only be the case when there are at least some genotypes in the population that invest in loners. In this case we can write

$$\begin{aligned} S_{\alpha,k+1} &= e^{-\delta(T_{k+1}+t^*_{k+1})} S_{\alpha,k} + \alpha e^{-\mu T_{k+1}} L_{\alpha,k} G(t^*_{k+1}) \\ L_{\alpha,k+1} &= (1-\alpha) e^{-\mu T_{k+1}} L_{\alpha,k} G(t^*_{k+1}) \end{aligned} \tag{10}$$

where for simplicity of notation we used $G(t^*_{k+1}) = G(t^*_{k+1}; e^{-\mu T_{k+1}} L_k; R_0)$, which is the growth of a cell before the resources are depleted, given that the initial number, $e^{-\mu T_{k+1}} L_k$, of cells is given by the number of surviving loners after starvation time T_k, and that the initial resource input is R_0. Notice that for the growth function we do not use an index α. This is because the initial conditions after starvation event k might contain loners of many different genotypes. Thus, when we say L_k we mean all loners, of all possible genotypes, after phase k. Note that, as mentioned above, t^* also depends on the initial conditions – however, to simplify the notation, since the initial conditions are the same as those in the argument of G, we simply use t^*.

(ii) the spores can complete their germination, in which case we can write:

$$\begin{aligned} S_{\alpha,k+1} &= \alpha \Big(e^{-\delta(T_{k+1}+\tau)} s S_{\alpha,k} + e^{-\mu T_{k+1}} L_{\alpha,k} G(\tau) \Big) G(t^*_{k+1}) \\ L_{\alpha,k+1} &= (1-\alpha) \Big(e^{-\delta(T_{k+1}+\tau)} s S_{\alpha,k} + e^{-\mu T_{k+1}} L_{\alpha,k} G(\tau) \Big) G(t^*_{k+1}) \end{aligned} \tag{11}$$

where as before, for simplicity, we denote $G(\tau) = G(\tau; e^{-\mu T_{k+1}} L_k; R_0)$ to be the growth of a cell during time τ, given that the initial population is made of the surviving loners and the initial resources are R_0. Similarly, $G(t^*_{k+1}) = G\big(t^*_{k+1}; e^{-\delta(T_{k+1}+\tau)} s S_k + e^{-\mu T_{k+1}} L_k G(\tau); R(\tau; e^{-\mu T_{k+1}} L_k; R_0)\big)$ is the growth of a cell in the time before resources are depleted, given that the new initial population size is given by the active spores that have survived starvation and successfully completed germination and the loners which have grown for time τ; the amount of resources available is that left from the initial R_0, after the loners have consumed food during time τ. Here, as well, the growth is determined by all genotypes in the population; hence the growth term does

not depend on the genotype α. Note that, as mentioned above, t^* also depends on the initial conditions – however, to simplify the notation, since the initial conditions are the same as those in the argument of G, we simply use t^*.

For different T_k this problem is hard (if not impossible) to solve analytically. However, when the environment is entirely deterministic (i.e. all starvation times have the same length) analytical results are possible. When all starvation periods have the same length T, our simulations show that the system converges to equilibrium values S^*_α, L^*_α and t^*. At this equilibrium, the system will either be such that we are in case (i) (loners finish the food before spores can germinate) or in case (ii) (spores can complete the germination process). If the former, then at equilibrium spores never get to germinate, but simply decay at rate δ; so it is trivial that the winning genotype will be one that does not invest in spores at all, i.e. $\alpha = 0$. The more interesting scenario occurs when at equilibrium we are in case (ii), so that genotypes that invest in spores can potentially have a benefit. In this case, we need to explore what strategies can be present at equilibrium. For this, we perform an analysis to assess what strategies are evolutionarily stable. At equilibrium, a resident monoculture population of type α will satisfy the following:

$$\begin{aligned} S^*_\alpha &= \alpha\Big(\overbrace{e^{-\delta(T+\tau)}}^{A} s\, S^*_\alpha + \overbrace{e^{-\mu T} G_\alpha(\tau)}^{B_\alpha} L^*_\alpha\Big) G_\alpha(t^*) \\ L^*_\alpha &= (1-\alpha)\Big(e^{-\delta(T+\tau)} s S^*_\alpha + e^{-\mu T} G_\alpha(\tau) L^*_\alpha\Big) G_\alpha(t^*) \end{aligned} \tag{12}$$

where the subscript α in $G_\alpha(\tau)$ and $G_\alpha(t^*)$ simply means that there is only one type in the population and where we denote $A = e^{-\delta(T+\tau)} s$ and $B_\alpha = e^{-\mu T} G_\alpha(\tau)$. The above equations imply that $S^*_\alpha / L^*_\alpha = \alpha/(1-\alpha)$ for $\alpha \neq 1$. When $\alpha = 1$ then $L^*_\alpha = 0$, as expected. Then from (12) we obtain that the growth of a cell before starvation in an environment where only type α is present is given by

$$G_\alpha(t^*) = \frac{1}{\alpha A + (1-\alpha) B_\alpha} \tag{13}$$

This holds for $\alpha \neq 1$; however, for $\alpha = 1$ we conclude directly from (12) that $S^*_1 = A G_1(t^*) S^*_1$, which implies that $G_1(t^*) = 1/A$. Thus, (13) holds for all $\alpha \in [0, 1]$.

If we introduce a very small population of an invader β into a resident population $\alpha \neq 1$, then the growth of β is described by the equations

$$\begin{aligned} S'_{\beta,\alpha} &= \beta\Big(AS_{\beta,\alpha} + B_\alpha L_{\beta,\alpha}\Big)G_\alpha(t^*) \\ L'_{\beta,\alpha} &= (1-\beta)\Big(AS_{\beta,\alpha} + B_\alpha L_{\beta,\alpha}\Big)G_\alpha(t^*) \end{aligned} \tag{14}$$

The subscript α signifies, as above, that the resident population is of type α. Since the invader genotype is introduced at very low levels, its immediate growth occurs in the environment where growth is still determined by the resident genotype, such that $G_\alpha(t^*)$ is in fact given by (13). The only exception is when $\alpha = 1$, i.e. the resident is all-spores. Then any genotype $\beta \neq 1$ will have loners that will be able to grow during time τ as if they were alone in the environment; thus, in this case, the growth in time τ is in fact $G_\beta(\tau)$ and not $G_1(\tau)$ and the matrix becomes

$$\begin{aligned} S'_{\beta,1} &= \beta\Big(AS_{\beta,1} + B_\beta L_{\beta,1}\Big)G_1(t^*) \\ L'_{\beta,1} &= (1-\beta)\Big(AS_{\beta,1} + B_\beta L_{\beta,1}\Big)G_1(t^*) \end{aligned} \tag{15}$$

Next we calculate in general the growth of genotype β in an α-monoculture; for $\alpha \neq 1$ this can be found from (14) to be $\lambda_{\beta,\alpha} = \beta A G_\alpha(t^*) + (1-\beta)B_\alpha G_\alpha(t^*)$, which can be further written as:

$$\lambda_{\beta,\alpha} = \frac{\beta A + (1-\beta)B_\alpha}{\alpha A + (1-\alpha)B_\alpha} \tag{16}$$

for $\alpha \neq 1$, while for $\alpha = 1$ we obtain from (15)

$$\lambda_{\beta,1} = \frac{\beta A + (1-\beta)B_\beta}{A} \tag{17}$$

We first explore when the pure strategies can invade or be invaded by other strategies.

(a) 0 is not invadable by strategy $\alpha \neq 0$ if and only if $\lambda_{\alpha,0} < 1$, which is equivalent to $A < B_0$. Since this latter condition is independent of α, we conclude that if $A < B_0$, then 0 is not invadable by any strategy $\alpha \neq 0$. Conversely, if $A > B_0$, then 0 is

invadable by all strategies.

(b) 0 can invade strategy α if and only if $\lambda_{0,\alpha} > 1$, which is equivalent to $A < B_\alpha$.

(c) 1 is not invadable by strategy $\alpha \neq 1$ if and only if $\lambda_{\alpha,1} < 1$, which is equivalent to $A > B_\alpha$.

(d) 1 can invade $\alpha \neq 1$ if and only if $\lambda_{1,\alpha} > 1$, which is equivalent to $A > B_\alpha$. If $A = B_\alpha$ then 1 and α are neutral with respect to each other.

From these conditions we conclude that a strategy α can be invaded by either strategy 0 (if $A < B_\alpha$) or by strategy 1 (if $A > B_\alpha$). Therefore, *an intermediate strategy α can never be an ESS and the only possible ESSes are the pure strategies.* (In the threshold case $A = B_\alpha$, 1 and α are neutral, so α is again not an ESS). Next we will show that there can be at most one ESS.

From (a) above, we know that 0 is ESS if $A < B_0$; using (c) this also means that 0 invades 1, which means that 1 cannot be an ESS. Similarly, if 1 is an ESS, then from (c) we know that $A > B_\alpha$ for all $\alpha \neq 0$; this implies that $A > B_0$ as well, which means that 0 cannot be an ESS. Thus, *there can be at most one ESS for a given set of parameters.* Notice that here we proved more than just ESS. The strategy that is ESS is not only stable against invasion, but it also invades all other strategies. Therefore, we have proved that the winning strategy is a continuously stable strategy (CSS).

Finally, we explore whether there can be no ESSes (i.e. whether neither of the pure strategies is an ESS). One possibility occurs when 0 and 1 are neutral with each other, i.e. $A = B_0$. In that case we find the critical starvation time threshold

$$T_{\rm cr} = \frac{\log(G(\tau)) - \log s + \delta\tau}{\mu - \delta} \tag{18}$$

such that if $T < T_{\rm cr}$ then 0 is an ESS and if $T > T_{\rm cr}$ then 1 is an ESS (Fig. S2A).

Another possibility for there not to be any ESS is if $A \geq B_0$ (i.e. 0 is not an ESS) and $A < B_\alpha$ for some $\alpha \in (0, 1)$ (i.e. 1 is not an ESS). However, we conjecture and confirm via simulations for the parameters of interest in this paper that for biologically relevant parameter regimes either 0 or 1 will be an ESS, except when these are neutral to each other.

This last case is given by (18).

From equation (18) it is also easy to see how the parameters of our model affect the threshold T_{cr}: the right hand side of the above equation is decreasing in s and μ and increasing in τ, δ and $G(\tau)$, the latter of which is an increasing function of the resource input R_0, an increasing function of the consumption rate c and a decreasing function of $R_{1/2}$. Thus, we conclude that loners are favored for decreasing spore success rate s, decreasing loner mortality rate μ, and decreasing $R_{1/2}$ and for increasing time to germination τ and increasing spore mortality rate δ. Finally, we treat the size of the resource pulse, R_0, separately. If the resource pulse is fixed, then the higher it is, the easier it is to select for loners. Varying R_0 has a sigmoidal effect on T_{cr} for deterministic T (Fig S.4), suggesting that for low and high values of the resource pulse the benefit of increasing R_0 is only marginal. Thus, since T is exponentially distributed, the benefits of varying R_0 in a stochastic environment are marginal and the resulting ESS α varies little with varying resource pulse size.

Finally, a more realistic scenario is that the resource pulse is stochastic. Our simulations suggest that introducing stochasticity in the resource pulse size does not select for mixed investment in loners and spores: if the starvation time T is fixed and the only source of stochasticity comes from the resource pulse, our simulations find that the only evolutionarily stable strategies are the pure strategies. However, because this is only a simulation result, it is possible that for different parameter combinations resource stochasticity will result in mixed investment. The relationship between the resource pulse and the time to starvation is an interesting one and needs to be further explored, for different distributions of resources and stochastic times; however, since our preliminary analysis suggests that the more interesting and rich behavior seems to be induced by the starvation times, in this paper we choose to perform the entire analysis for a fixed resource input following every starvation period. A full sensitivity analysis for stochastic T is shown in Fig. S3.

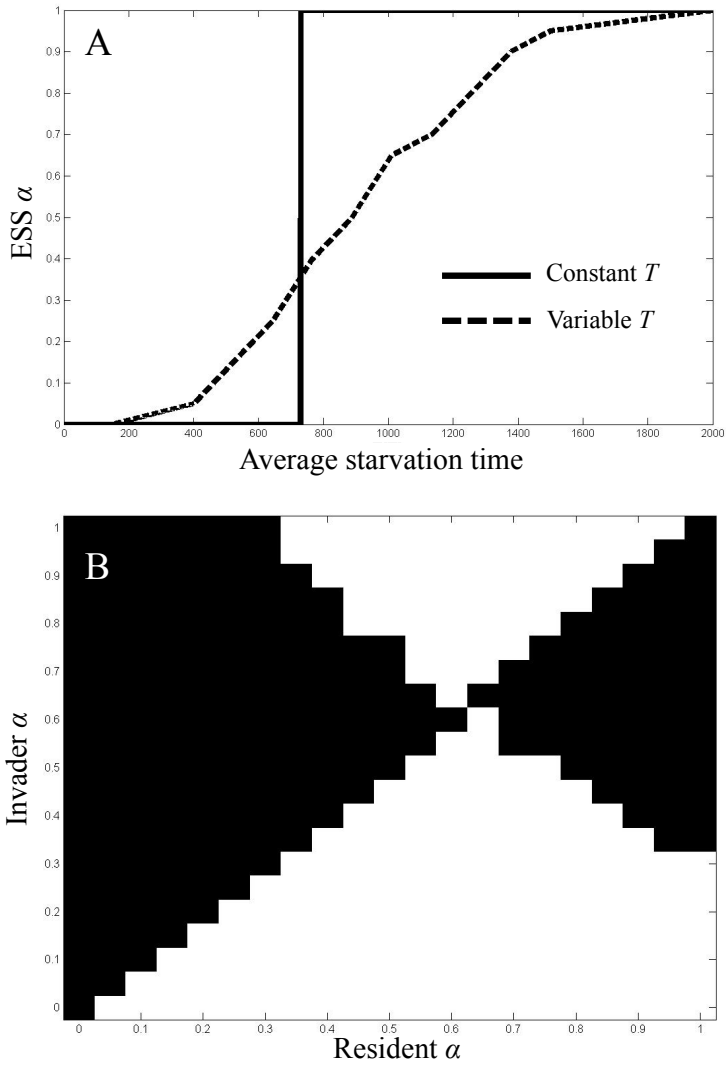

Fig. S 2 – In one environment, deterministic (fixed) starvation times always select for pure strategies while stochastic starvation times can select for mixed strategies. **A.** The α corresponding to the continuously stable strategy (CSS) is shown as a function of average starvation time for both deterministic and stochastic cases. In the deterministic case, if $T < T_{\rm cr}$, then the all-loners strategy wins; if $T > T_{\rm cr}$, then the all-spores strategy wins. In the stochastic case, extreme average starvation times select for the corresponding pure strategies, but intermediate average starvation times select for mixed strategies (intermediate α). **B.** The pairwise invasibility analysis shows that the winning strategy is not only stable against invasion, but also able to invade all other strategies from rare. Therefore, our winning strategy is continuously stable (CSS). The pairwise invasibility plot (PIP; the black squares show for each resident trait value all mutant trait values which can invade) for the stochastic case with average starvation time $\lambda_T = 1000$. The CSS strategy is $\alpha = 0.63$, which invests 63% in spores and 37% in loners.

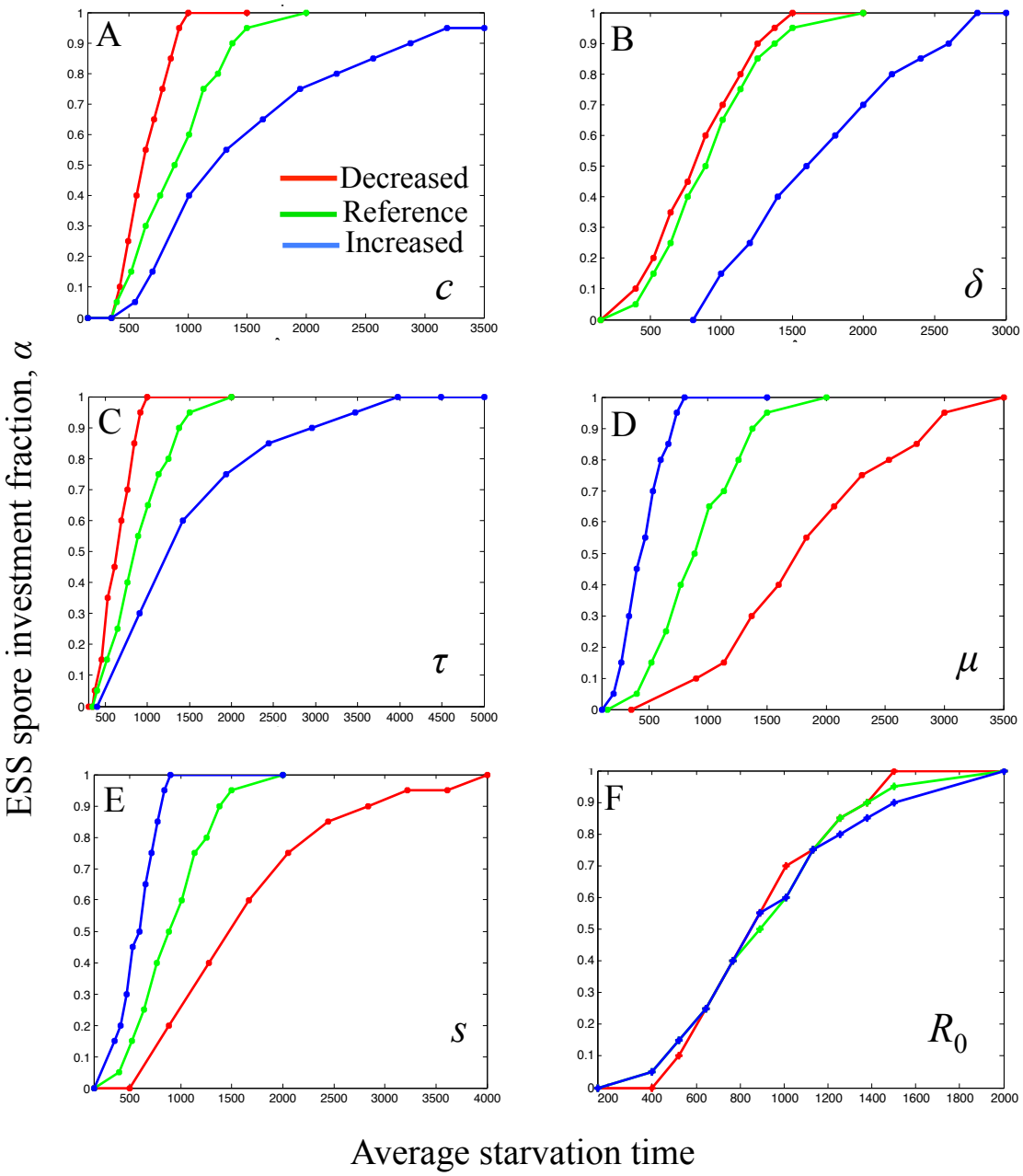

Fig. S 3 – The sensitivity of the model to the parameters. **A, B, C, F.** Higher consumption rate (c), spore death rate (δ), time needed for spore germination (τ) or resource input favor selection for loners. **D, E.** Conversely, higher loner decay rate (μ) or higher spore survival and viable germination rate (s) favor selection for spores. In all panels, the green curve corresponds to the reference value of the parameter, as found in Table S1; red corresponds to a decreased value of the parameter under study; blue corresponds to an increased value. Except for the parameter varied to perform the sensitivity analysis, all other parameters are as in Table S1. Parameter values for the sensitivity analysis: $c = 0.086,\ 0.173,\ 0.346$; $\delta = 0.00004,\ 0.0002,\ 0.001$; $\tau = 2,\ 4,\ 8$; $\mu = 0.001,\ 0.002,\ 0.004$; $s = 0.25,\ 0.5,\ 0.75$; $R_0 = 104,\ 108,\ 1012$.

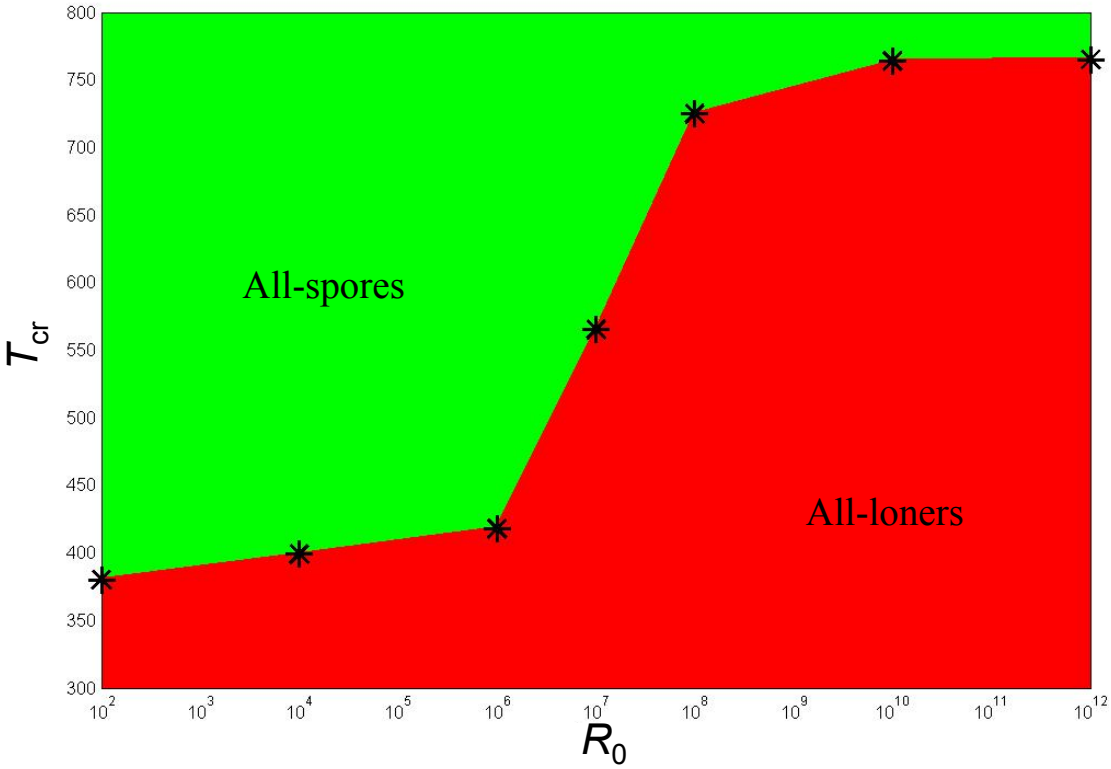

Fig. S 4 – Varying R_0 has a sigmoidal effect on the threshold $T_{\rm cr}$: low values of R_0 lead to low threshold values and thus favor spores; high values of R_0 lead to high threshold values and thus favor loners; in between, for a narrow range of intermediate values, there is a sudden jump. Green = all-spores; red = all-loners. All parameters are as in Table S1.

2 Details of the simulations

We performed numerical simulations of $M = 25$ patches undergoing desynchronized growth-starvation cycles. The patches were chosen with mean starvation times $\lambda_T = 80i$, $i = 1, \ldots, 25$. The spectrum of genotypes was discretized: we used 21 strategies ($\alpha_i = 0.05i$, $i = 0, \ldots, 20$) corresponding to a regular discretization of step 0.05 (Figure 3 in the main text). We found however that this discretization leads to the artifact that in fast environments the strategy $\alpha = 0.05$ might be selected for and dispersed to artificially invade slower environments. Therefore we performed additional simulations using a finer mesh for those strategies favoring the existence of loners. We used $\alpha_i = 0.01i$, $i = 0, \ldots, 10$ and $\alpha_i = 0.05i$, $i = 3, \ldots, 20$, so 29 genotypes were considered (Fig. S5) to show that a finer mesh makes the artifact disappear: $\alpha = 0.05$ is not selected for but instead $\alpha = 0.01$ is selected for in Fig. S5; if an even finer mesh would be considered, the fine band of color around $\alpha = 0.01$ would move even closer to $\alpha = 0$ and would be less and less represented in (to the point of disappearing from) the fast environments.

Initial abundances of each genotype were independently drawn from a standard log-normal distribution and subsequently normalized so that the entire population contained 10^8 cells in every environment. The cells of the different genotypes were then split into spores with probability α_i and loners with probability $1 - \alpha_i$. An initial resource pulse of magnitude 10^8 was added and the trajectories governed by equations (1) were integrated using finite-differences numerical methods. In the simulations, dispersal took place at the end of the growth phase in a given environment (i.e., when the resources crossed R^*). Firstly, the population of each genotype was divided between spores and loners depending on α and secondly, a fraction D of the successfully formed spores was equally distributed among the rest of the environments. Since only a fraction s of spores are viable upon germination, each patch receives a pulse of $sD\alpha_i/(M-1)$ spores, while a fraction $s\alpha_i(1-D)$ of each genotype stays at the home patch. The starvation phase starts then in the dispersing environment, with a duration T_k drawn from an exponential distribution with mean λ_T. During this period spore populations decayed exponentially at rate δ while loners decayed exponentially at rate

$\mu > \delta$. At the end of the starvation time we measured the abundance of each genotype and a new resource pulse of size 10^8 arrived. To obtain Figure 3 in the main text as well as Figure 5 simulations were run for 1500 growth/starvation cycles in the slowest patch, which means, on average 3×10^6 hours.

Dispersed spores arriving to depleted patches remained dormant until a new pulse of resources arrived, then after a time τ, they became active loners if resources were still available. Otherwise they stayed unaffected, representing no cost to spores aborting germination. On the other hand, dispersed spores arriving during a growth phase started the maturation phase upon arrival.

Invasion Analysis. MATLAB R2013b. ode15s and the parallel computing toolbox was used to perform the invasions and the sensitivity analysis. Residents were established at an initial abundance of 10^8 and invaders with initial abundance equal to a half that of the resident. Single patch growth-starvation cycles were run for 1000 cycles and replicated 4 times. If the invader had, on average across replicates, a higher abundance than the resident at the end of the 1000th growth phase, the corresponding square in the pairwise invasibility plot (PIP) was colored black, otherwise the corresponding square was colored white. The diagonal entries, where residents and invaders were neutral, were not simulated but instead set to black as a default.

Sensitivity analysis. Parameters c, μ, δ, τ, s and R_0 were varied to study their effects. Our estimates of α_{ESS} and α^*, were obtained by running 20 replicate single-patch simulations for 1000 growth/starvation cycles each, and finding the α_i with the highest abundance, on average across replicates.

Coexistence analysis. The system was initialized as explained above. After 10^6 time units 90% of the population of either genotype $\alpha = 0.4$ or $\alpha = 0.9$ was removed and the evolution of that strategy in environments $\lambda_T = 80$, $\lambda_T = 720$, $\lambda_T = 1360$, $\lambda_T = 2000$ was tracked. The time series is shown with a 5000 time units sampling and the temporal average (dashed

Table of notation and parameter values

Parameter	Use	Value
c	consumption rate	0.173 (4-hour doubling time)
$R_{1/2}$	resource concentration at which the reaction rate is at half-maximum	10^7
R_0	resource input after starvation	10^8
s	fraction of aggregating cells that become viable spores	0.504
τ	time needed for spore germination	4 hours
μ	death rate of amoebae	0.002
δ	death rate of spores	0.0002
α, β	fraction of aggregating amoebae	variable
T	length of starvation	variable
λ_T	average length of starvation	variable

Table S 1 – Table of notations used in the text and the baseline parameter values used for simulations, unless otherwise specified in the figure legends.

thick line in Figures 9 and 10 obtained according to

$$\langle x \rangle_\tau = \int_{t-\tau/2}^{t+\tau/2} x(t')dt' \tag{19}$$

with $\tau = 10^6$.

References

[1] Michaelis L, Menten ML (1913) Die Kinetik der Invertinwirkung. *Biochem Z* 49: 333-369.

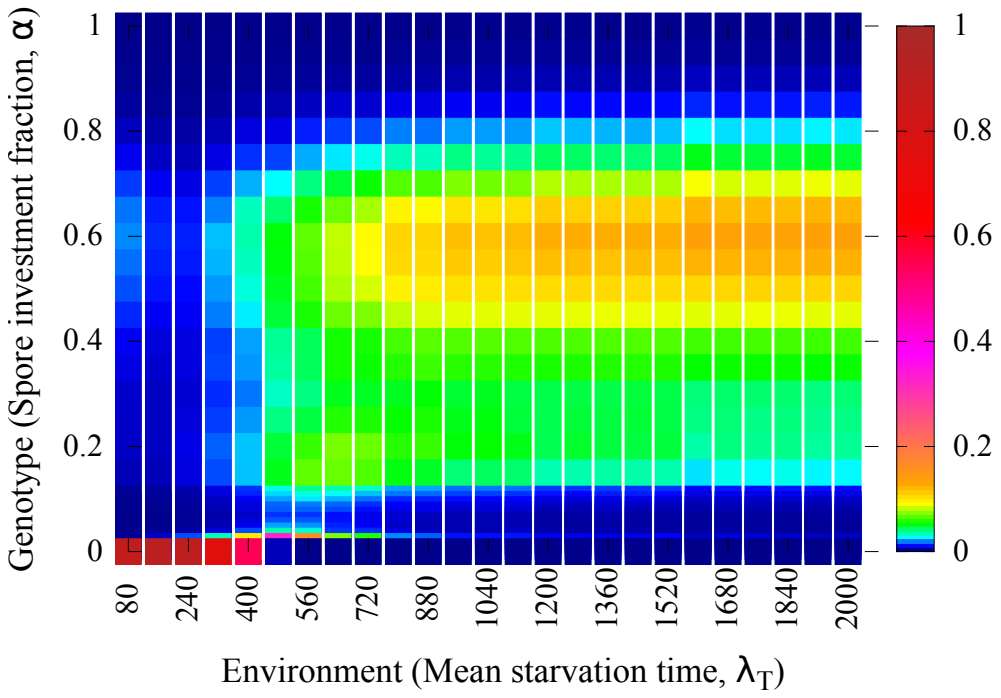

Fig. S 5 – Frequency of the 29 genotypes at the end of 1500 growth/starvation cycles in the slowest environment (3×10^6 hours on average). 25 environments coupled with a dispersal of $D = 0.6$ are considered. Details above and parameters as for Fig. 3 in the main text.

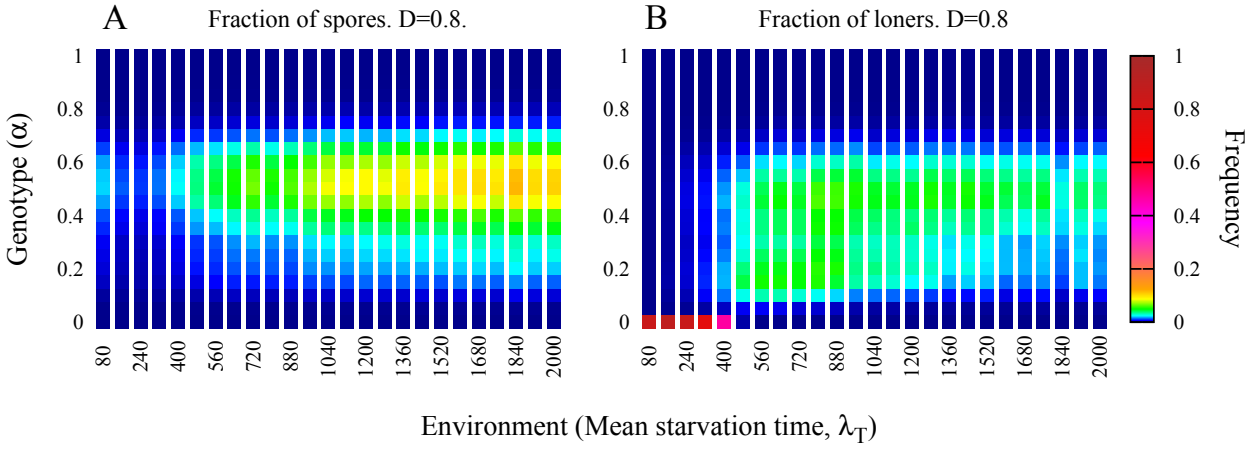

Fig. S 6 – Mean frequency of spores (A) and loners (B) across 25 environments. 21 genotypes ($\alpha = 0.05i$; $i = 0, ..., 20$) are considered coupled with a dispersal $D = 0.8$. Average is taken over 60 replicates after 1500 growth/starvation cycles in the slowest environment (3×10^6 hours on average). **A.** Spores of the bet-hedging strategy are more abundant in slower-recovery environments and seed faster-recovery environments through dispersal. **B.** Loners of $\alpha = 0$ dominate faster-recovery environments. Loners of any given genotype are more abundant than its spores in faster environments.

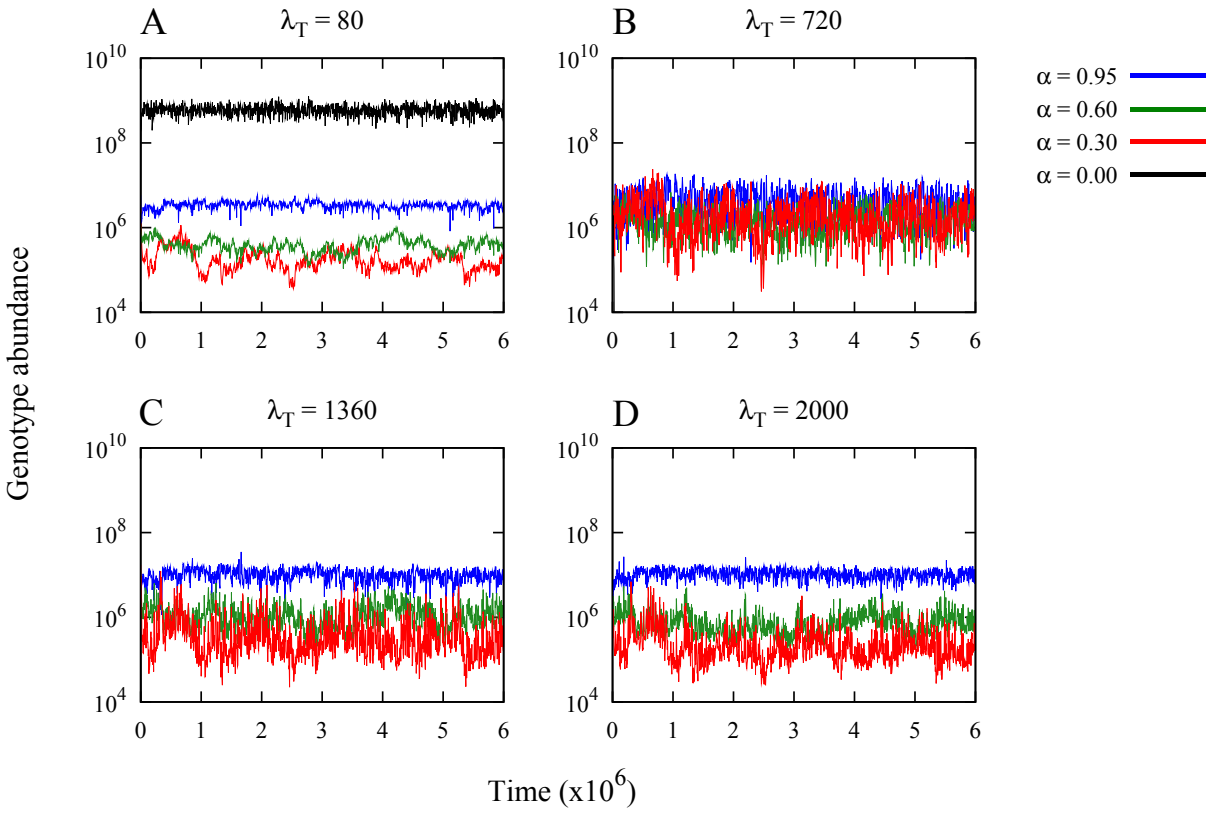

Fig. S 7 – (Log-linear plot). Long-time evolution of genotype abundance in one of the numerical simulations (Section 2). 25 environments were intialized with the 29 genotypes in each one. 4 representative genotypes [$\alpha = 0.95$ (blue), $\alpha = 0.6$ (green), $\alpha = 0.3$ (red) and $\alpha = 0$ (black)] in 4 of the environments: **A.** $\lambda_T = 80$, **B.** $\lambda_T = 720$, **C.** $\lambda_T = 1360$, **D.** $\lambda_T = 2000$ are shown. The trajectories were sampled each 5000 time units. Dispersal intensity $D = 0.1$. Fast environments (A) favor the presence of loners although other genotypes are also present. Slower patches (B, C, D) allow the coexistence of several genotypes with higher abundance of strategies that favor the formation of spores (see Fig. 3 in the main text).

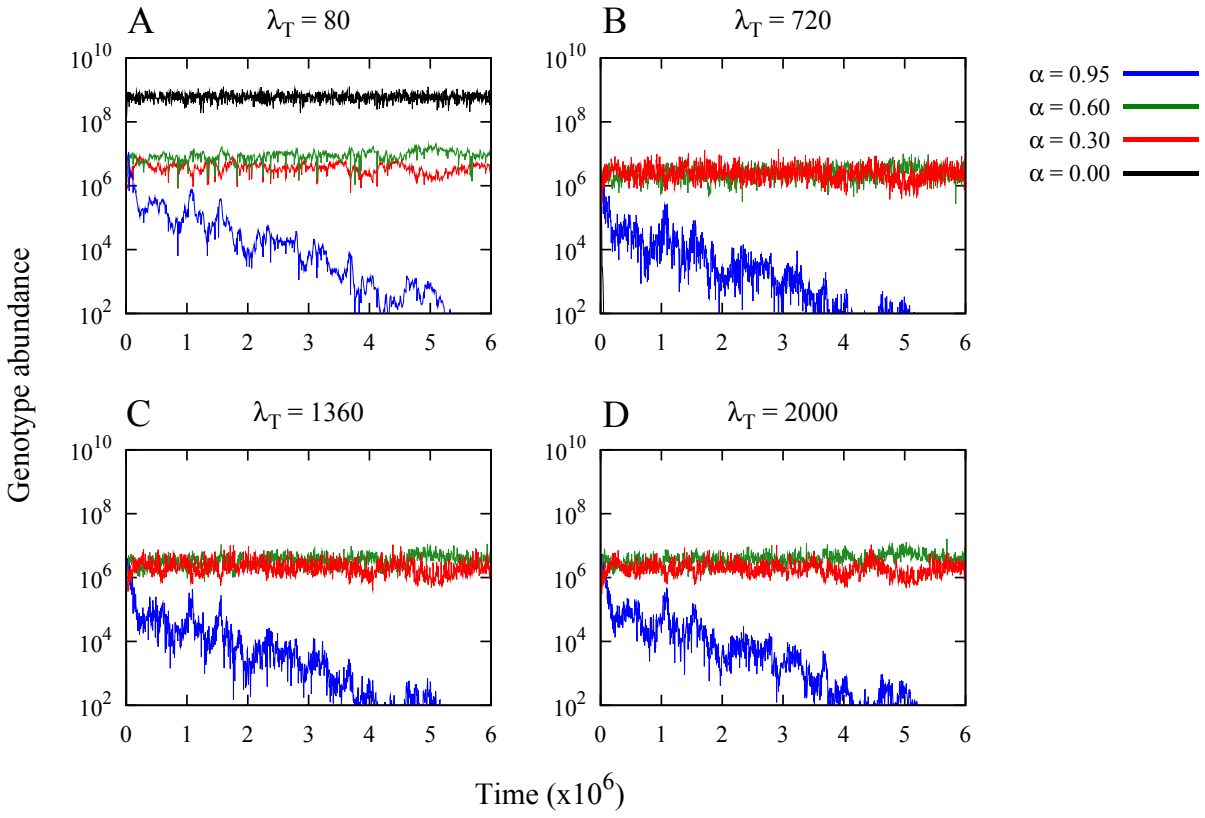

Fig. S 8 – (Log-linear plot). Long-time evolution of genotype abundance in one of the numerical simulations (Section 2). 25 environments were initialized with the 29 genotypes in each one. The Figure shows 4 representative genotypes [$\alpha = 0.95$ (blue), $\alpha = 0.6$ (green), $\alpha = 0.3$ (red) and $\alpha = 0$ (black)] in 4 of the environments: **A.** $\lambda_T = 80$, **B.** $\lambda_T = 720$, **C.** $\lambda_T = 1360$, **D.** $\lambda_T = 2000$ are shown. The trajectories were sampled each 5000 time units. Dispersal intensity $D = 0.8$. Fast environments (A) are almost not affected by dispersal and favor strategies with a high investment in loners. Strategies favoring the formation of spores do not survive. On the contrary, increasing dispersal makes all faster environments select for mixed strategies (see Fig. 3 in the main text).

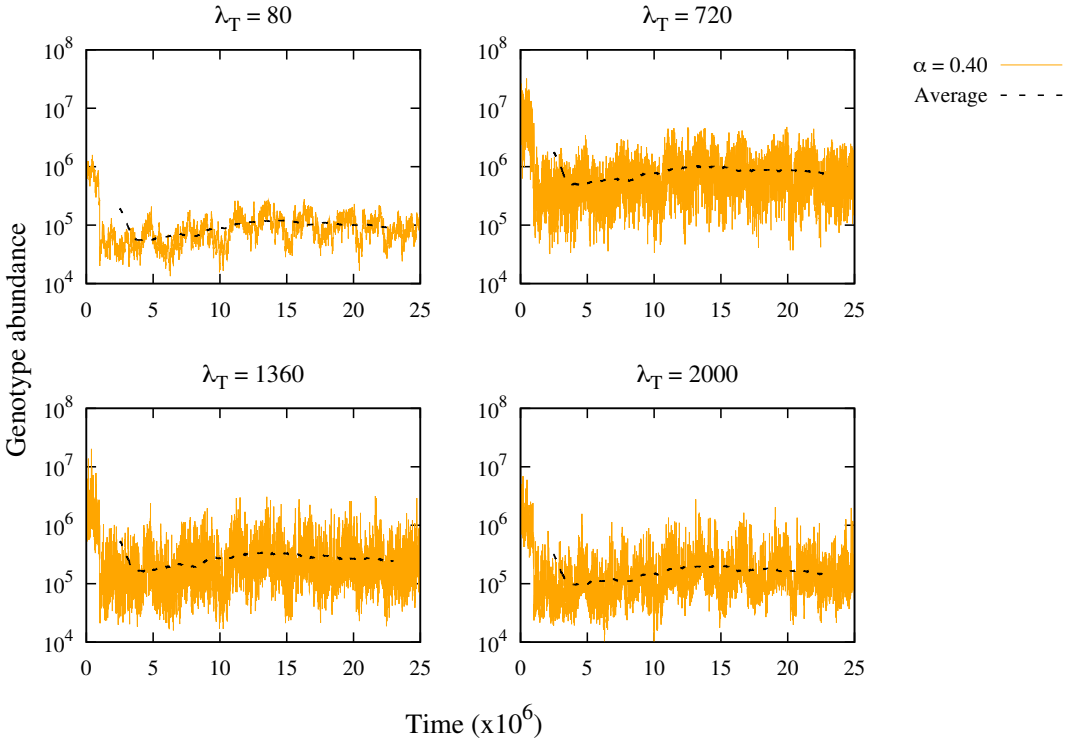

Fig. S 9 – (Log-linear plot). Temporal evolution of the genotype $\alpha = 0.4$ (low abundance, color ranging from dark-blue to green across environments in Fig. 3, main text) after removing 90% of its total population (i.e. in all environments) at time $t = 10^6$. The recovery of the population is shown in 4 of the environments **A.** $\lambda_T = 80$, **B.** $\lambda_T = 720$, **C.** $\lambda_T = 1360$, **D.** $\lambda_T = 2000$. The trajectories are sampled every 5000 time units. $D = 0.1$. The thick dashed line is the temporal average (Section 2 for details).

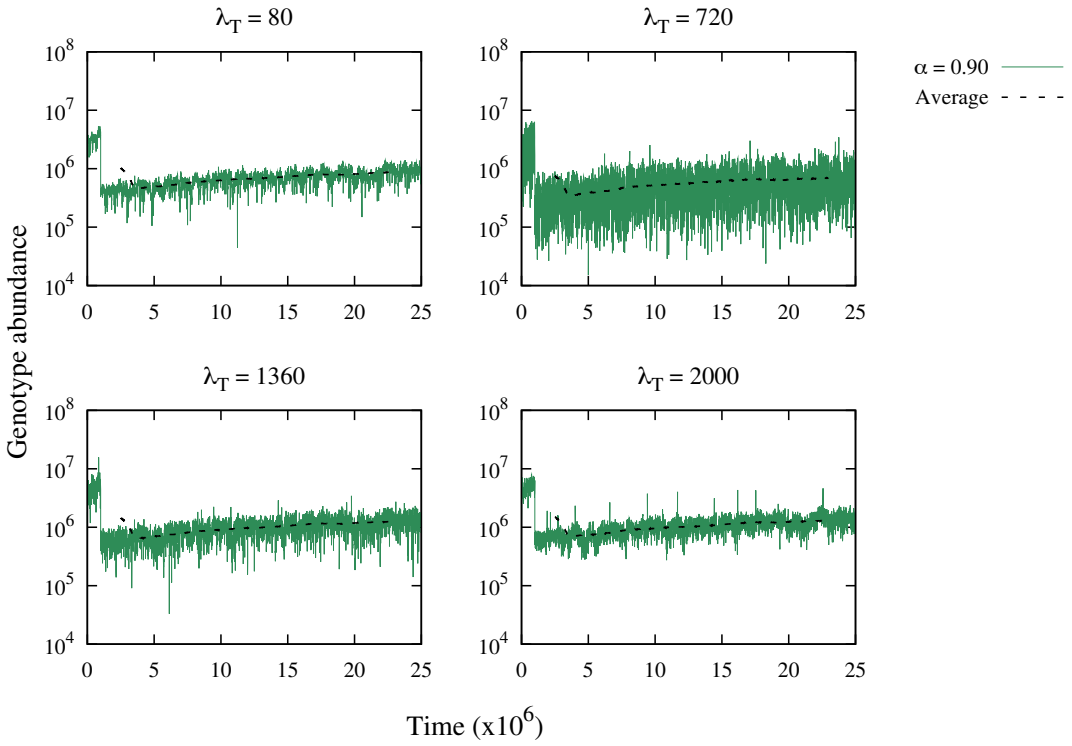

Fig. S 10 – (Log-linear plot). Temporal evolution of the genotype $\alpha = 0.9$ (low-medium abundance, color ranging from blue to yellow in Fig. 3, main text) after removing 90% of its total population at time $t = 10^6$ (thin dashed line). The recovery of the population is shown in 4 of the environments **A.** $\lambda_T = 80$, **B.** $\lambda_T = 720$, **C.** $\lambda_T = 1360$, **D.** $\lambda_T = 2000$ is shown. The trajectories are sampled every 5000 time units. $D = 0.2$. The thick dashed line is the temporal average (Section 2 for details).